J. Am. Soc. Mass Spectrom. (2017) 28:2716–2723
DOI: 10.1007/s13361-017-1805-x

RESEARCH ARTICLE

New Features in the Lipid A Structure of *Brucella suis* and *Brucella abortus* Lipopolysaccharide

Adriana C. Casabuono,[1] Cecilia Czibener,[2] Mariela G. Del Giudice,[2] Ezequiel Valguarnera,[2] Juan E. Ugalde,[2] Alicia S. Couto[1]

[1]Universidad de Buenos Aires, Facultad de Ciencias Exactas y Naturales, Departamento de Química Orgánica - Consejo Nacional de Investigaciones Científicas y Técnicas, Centro de Investigación en Hidratos de Carbono (CIHIDECAR), Ciudad Universitaria, Intendente Güiraldes 2160, C1428GA, Buenos Aires, Argentina
[2]Instituto de Investigaciones Biotecnológicas "Dr. Rodolfo A. Ugalde", IIB-INTECH, CONICET, Universidad Nacional de San Martín, San Martín, Buenos Aires, Argentina

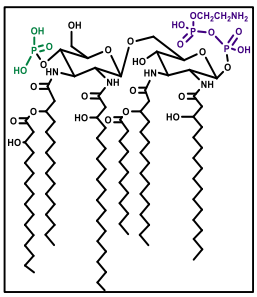

Abstract. Brucellaceae are Gram-negative bacteria that cause brucellosis, one of the most distributed worldwide zoonosis, transmitted to humans by contact with either infected animals or their products. The lipopolysaccharide exposed on the cell surface has been intensively studied and is considered a major virulence factor of *Brucella*. In the last years, structural studies allowed the determination of new structures in the core oligosaccharide and the O-antigen of this lipopolysaccharide. In this work, we have reinvestigated the lipid A structure isolated from *B. suis* and *B. abortus* lipopolysaccharides. A detailed study by MALDI-TOF mass spectrometry in the positive and negative ion modes of the lipid A moieties purified from both species was performed. Interestingly, a new feature was detected: the presence of a pyrophosphorylethanolamine residue substituting the backbone. LID-MS/MS analysis of some of the detected ions allowed assurance that the Lipid A structure composed by the diGlcN3N disaccharide, mainly hexa-acylated and penta-acylated, bearing one phosphate and one pyrophosphorylethanolamine residue.

Keywords: Brucella, Lipopolysaccharide, Lipid A, MALDI-TOF MS

Received: 6 July 2017/Revised: 18 August 2017/Accepted: 26 August 2017/Published Online: 18 September 2017

Introduction

Brucellaceae are gram-negative, facultative, intracellular bacteria that cause brucellosis, one of the most distributed worldwide zoonosis, transmitted to humans by contact with either infected animals or their products. They cause an acute or chronic disease with a wide range of symptoms, and difficult to diagnose and treat [1]. The species with the highest zoonotic potential are *B. abortus*, responsible for bovine brucellosis, *B. melitensis*, the main etiologic agent of ovine and caprine brucellosis, and *B. suis*, responsible for swine brucellosis [2, 3].

The lipopolysaccharide (LPS) is considered to be a major virulence factor of *Brucella* and it induces a strong antibody response during infection or when whole cell vaccines are used [4, 5]. LPSs are exposed on the cell surface and present three different regions with different chemical and biological properties: the lipid A, the core oligosaccharide, and the polysaccharide, which in most cases represents the O-specific polysaccharide (O-PS, O-antigen) [6, 7]. The LPS of *Brucella* shows very low endotoxicity, which illustrates poor detection by the innate immune system and is considered to be one of the virulence factors that allows the pathogen to escape detection by the host immune system [4, 8].

The structure of the polysaccharide chain of the LPS of *B. abortus, B. melitensis*, and *B. suis* has been studied [9–11]. In all cases it was described as a homopolymer of 4-formamido-4,6-dideoxy-D-mannose (*N*-formylperosamine, Rha4NFo), comprising two antigenic determinants named A (from *abortus*) and M (from *melitensis*). Epitope A was defined as a polymer of 1-2-linked *N*-formylperosamine (Rha4NFo), whereas epitope M was ascribed to the presence of some amounts of 1-3-linkages between perosamine residues. The highest concentration of M-epitope was found in the O-chain of *B. melitensis* strain 16 M and the following pentasaccharide repeating unit was suggested for epitope M: [–2-α-D-Rha4NFo-2-α-D-Rha4NFo-3-α-D-Rha4NFo-2-α-D-Rha4NFo-2-α-DRha4NFo–] [12]. More recently, a reinvestigation of both types of structures by 2D NMR showed that the M-epitope is a tetrasaccharide, missing one of

Correspondence to: Alicia S. Couto; *e-mail:* acouto@qo.fcen.uba.ar

the 2-linked Rha4NFo compared with the previously proposed structure. It was also determined that the polysaccharide from *B. melitensis* 16 M contains a fragment of 1-2- linked polymer, capped with M-type polymer and other strains containing one or two M-type units at the nonreducing end of the 1-2-linked O-chain [13]. Regarding the core oligosaccharide, the analysis of a *wadC* mutant suggested that the *B. abortus* LPS core presents a branched structure [14]. In a more recent structural study, the first chemical and spectroscopic analysis of its structure [15] and the identification of a new glycosyltransferase gene [16] confirmed the branched structure. Furthermore, a structural study of the LPS purified from *B. melitensis* defective mutants also identified a branched core oligosaccharide critical in virulence [17].

It is known that the hydrophobic lipid A region constitutes most of the outer leaflet of the outer membrane and is responsible for many of the endotoxic properties attributed to LPSs [18]. The first studies by thermotropic phase behavior [19] and immunochemical analysis [20] of *B. abortus* and *B. melitensis* lipid A suggested the presence of a disaccharide backbone molecule linked in a β1–6 configuration. Ethanolamine, neutral sugars, and ester-linked acyl-oxyacyl fatty acids were not detected, and phosphate was described as absent or present in reduced quantities [21]. Later, a structural analysis of the lipid A from *B. abortus* LPS, purified by HPLC was performed. Mono- and bisphosphoryl species containing a β-1-6-linked 2,3-diamino-2,3-dideoxy-(diaminoglucose) disaccharide backbone (diGlcN3N), substituted mainly with hydroxylated C16, C14, and C12 fatty acids and C16 or C18 in acyloxyacyl linkages, were characterized [22]. More recently, the lipid A profiles of R and S *Brucella abortus* strains were compared with *Escherichia coli* lipid A by mass spectrometry analysis, and the differences detected were ascribed to the presence mainly of hepta-acylated species in *Brucella* and hexa-acylated residues in *E. coli* lipid A [23].

It has been claimed that determination of the intrinsic heterogeneity in *Brucella* LPS is important to explain in a realistic perspective its chemical nature and biological behavior. This is significant, since the LPS is the most relevant antigen during infection and vaccination, and LPS/LPS-related molecules are extensively used in immunological studies as well as in the diagnosis of brucellosis [2]. Therefore, in this work we have reinvestigated the lipid A structure isolated from *B. suis* and *B. abortus* LPSs. Interestingly, a detailed study by MALDI-TOF mass spectrometry of the lipid A moieties purified from both species allowed detection of a new, interesting feature: the presence of a mainly hexa-acylated and penta-acylated diGlcN3N backbone substituted with a pyrophosphorylethanolamine residue.

Experimental

Bacterial Strains

Brucella abortus 2308 [24] and *Brucella suis* 1330 [25] were used as the strains to purify the LPS. Work with *Brucella* was performed at the Biosafety Level 3 laboratory facility at the Universidad Nacional de San Martín.

Growth of Bacteria and Isolation of the LPS

All *Brucella abortus* strains were cultured in tryptic soy broth (TSB) for 16–20 h at 37 °C with orbital shaking (250 rpm) or in solid media plates with the addition of nalidixic acid at 5 μg/mL.

LPS was extracted from *B. abortus* strains using a modification of the phenol-hot water method [26]; 250 mL of stationary cultures were washed twice with PBS pH 7.4 and resuspended at 100 mg of bacteria per mL of PBS. The suspension was autoclaved at 121 °C for 30 min and centrifuged 15 min at 5000 rpm. Supernatant was ultracentrifuged for 6 h at 40,000 rpm, and the pellet was resuspended in 100 mM Tris-HCl pH 7 with 20 μg/mL of DNase and RNase and incubated for 30 min at 37 °C. The sample was treated with 50 μg/mL Proteinase K for 3 h at 37 °C and 50 μg/mL Proteinase K was further added and incubated overnight at room temperature. The last two steps were repeated and the preparation was precipitated with 2 volumes of methanol with 1% sodium acetate-saturated methanol and incubated at least 1 h at –20 °C before centrifugation for 15 min at 5000 × *g* (4 °C). The pellet was resuspended in MilliQ water and dialyzed on MilliQ water at least overnight before ultracentrifugation for 6 h at 40,000 rpm. Pellet was resuspended in 1.5 mL of MilliQ water and extracted with PCP (phenol:chloroform:petroleum ether) as described. LPS was obtained from the phenol phase and the water-phenol interphase. Both phases were combined, washed with methanol, and resuspended in 0.1 mM $MgCl_2$ in MilliQ water. LPS was ultracentrifuged for 16 h at 15 °C and the pellet was resuspended in 1 mL of MilliQ water. LPS concentration was determined by the 3-deoxy-D-manno-2-octulosonic acid method [27]. Purified LPS was analyzed on 12% SDS-PAGE gels and stained by silver nitrate.

Isolation and Purification of Lipid A

LPS was hydrolyzed with 2% acetic acid for 3 h at 100 °C. Precipitated lipid A was recovered by ultracentrifugation at 4 °C, 10,000 *g* for 60 min. The solution containing the sugar moiety was separated and lyophilized rendering the oligosaccharide. The precipitated lipid A was washed with water, lyophilized, and further extracted with $CHCl_3$/MeOH 3:1 (v/v). The organic phase was dried to obtain purified lipid A.

UV-MALDI-TOF Mass Spectrometry Analysis

Matrices and calibrating chemicals were purchased from Sigma-Aldrich. Measurements were performed using an Ultraflex II TOF/TOF mass spectrometer equipped with a high performance solid-state laser (λ = 355 nm) and a reflector. The system was operated by the Flexcontrol 3.3 software package (Bruker Daltonics GmbH, Bremen, Germany).

The MALDI-TOF MS spectra were the result of 1000–1500 laser shots. All samples were measured in the linear and the reflectron mode, and as routine in both positive and negative

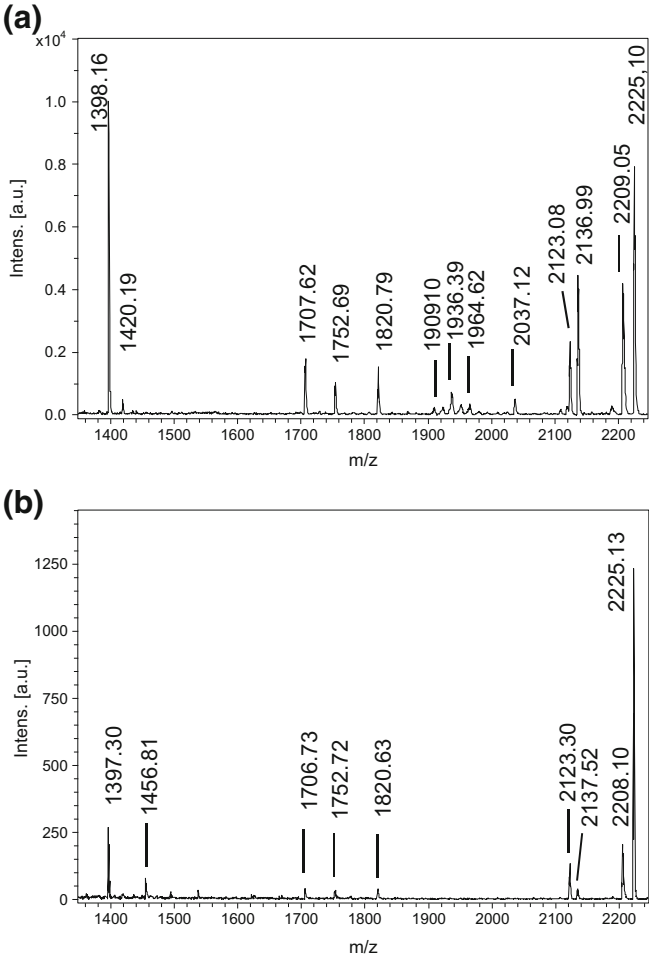

Figure 1. MALDI-TOF mass spectra acquired in the positive ion mode using gentisic acid as matrix. **(a)** Mass spectrum of *B. suis* lipid A. **(b)** Mass spectrum of *B. abortus* lipid A

polarity. Laser power was typically 40%–60% of its maximum intensity for mass spectra, and the accelerating voltage 20 kV.

For all experiments using the tandem-time-of-flight LIFT mode, the ion source voltage was set at 8.0 kV with a precursor ion mass window of 3 Da. Precursor ions generated by LID (laser-induced dissociation) were accelerated at 19.0 kV in the LIFT cell. The reflector voltage was set at 29.5 kV.

The samples were loaded onto a ground steel sample plate (MTP 384 ground steel; Bruker Daltonics GmbH) using the sandwich method or by the classic dried-droplet method: a sample/matrix solution mixture (1 mL, 1:1, v/v) was deposited on the target plate and allowed to dry under ambient conditions. In addition, different matrices were assayed. Best spectra were obtained using gentisic acid.

Results and Discussion

First, to elucidate the structures the LPS from *Brucella suis* wild type in order to compare it with *Brucella abortus* wild type, acid hydrolysis with acetic acid was performed on the corresponding LPSs to split the lipid A from the oligosaccharide. The corresponding lipids A were purified and analyzed by UV-MALDI-TOF mass spectrometry.

Mass spectrum of the lipid A obtained from *B. suis* LPS was acquired in the positive ion mode using GA as matrix (Figure 1a). The ions at *m/z* 2225.10 ($C_{112}H_{216}N_5Na_3O_{27}P_3^+$), *m/z* 2209.05 ($C_{114}H_{222}N_5NaO_{27}P_3^+$), *m/z* 2136.99 ($C_{110}H_{214}N_5NaO_{26}P_3^+$), and *m/z* 2037.12 ($C_{104}H_{202}N_5NaO_{25}P_3^+$) were attributed to the hexa-acylated diGlcN3N backbone substituted with one phosphoryl (P) and one pyrophosphorylethanolamine (PPEA) group. Furthermore, the ion at *m/z* 2123.08 ($C_{112}H_{216}N_5Na_2O_{24}P_2^+$) corresponds to *m/z* 2225.10 minus a sodium phosphoryl group. In the region *m/z* 1850–1700, three main signals were detected. The signals at *m/z* 1820.79 ($C_{94}H_{182}N_4NaO_{23}P_2^+$) and *m/z* 1752.69 ($C_{96}H_{185}N_4NaO_{19}P^+$) correspond to penta-acylated species carrying a diphosphoryl and monophosphoryl diGlcN3N backbone, respectively. The ion at *m/z* 1707.62 ($C_{82}H_{160}N_4Na_2O_{23}P_3^+$) was attributed to a tetra-acylated diGlcN3N backbone substituted with a pyrophosphoryl and a phosphoryl group, and the major ion at *m/z* 1398.16 ($C_{74}H_{143}N_4NaO_{16}P^+$) corresponds to a monophosphoryl tetra-acylated species (Table 1). When the mass spectrum of the lipid

Table 1. Proposed structures for lipid A obtained from *Brucella suis* LPS after MALDI-TOF mass spectrometry analysis in the positive ion mode. Sugar backbone: [GlcN3N-GlcN3N]

$Mass_{calc.}$ [a] $[M+Na]^+$	$Mass_{meas.}$ [b] $[M+Na]^+$	Proposed structures	P	EtN
2225.4589	2225.15	C12:0, 3 x C16 (3-OH),C18(3-OH), C20 (3-OH), 2 x Na	3	1
2209.5265	2209.06	C12:0, 2 x C16 (3-OH), 2 x C18(3-OH), C20 (3-OH)	3	1
2137.4688	2136.99	C10:0, C16:0, 2 x C16(3-OH), C18 (3-OH), C20 (3-OH)	3	1
2123.5106	2123.08	C12:0, 3 x C16 (3-OH), C18 (3-OH), C20 (3-OH), Na	2	1
2037.3799	2037.12	C12:0, 2 x C16:0, C14 (3-OH), 2 x C16 (3-OH)	3	1
1936.3528	1936.39	C12:0, 2 x C16:0, C14 (3-OH), 2 x C16 (3-OH), Na	2	-
1820.2568	1820.79	C14:0(OH), 3 x C16 (3-OH), C20 (3-OH)	2	-
1752.3268	1752.69	C18:0, C14:0 (3-OH), 2 x C16:0(3-OH), C20:0 (3-OH)	1	-
1708.0482	1707.62	C18:0, 2x C16:0(3-OH), C20:0 (3-OH), Na	3	-
1398.0134	1398.16	C12:0, C18:0, 2 x C16 (3-OH)	1	-

[a]calc: calculated monoisotopic masses.
[b]meas: measured.
GlcN3N: 2,3-diamino-2,3-dideoxyglucose; P: phosphate; EtN: ethanolamine.

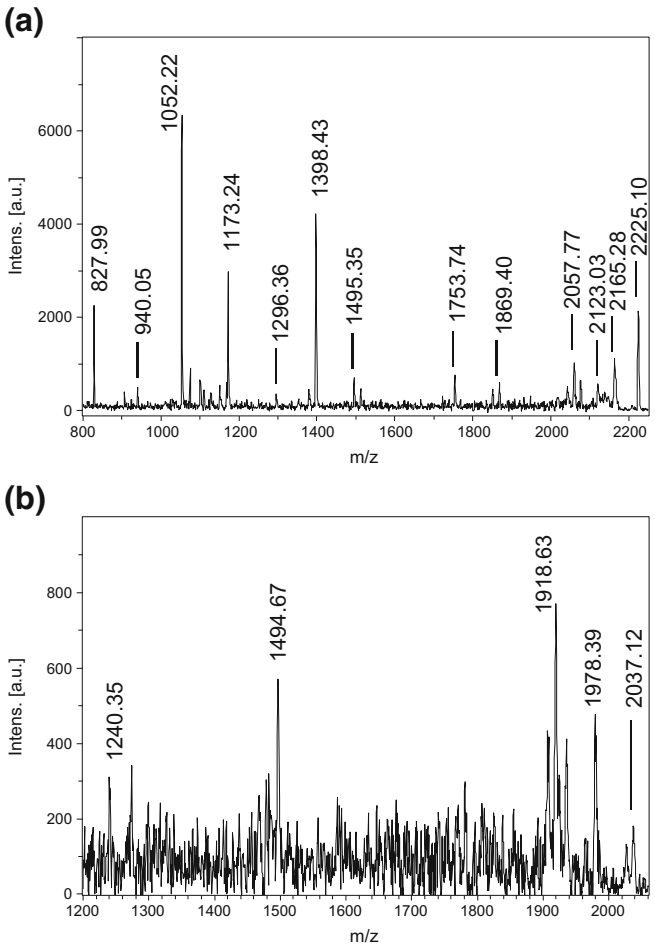

Figure 2. **(a)** LID-MS/MS spectrum of parent ion *m/z* 2225.10 from Figure 1. **(b)** LID-MS/MS spectrum of parent ion *m/z* 2037.12 from Figure 1

A obtained from *B. abortus* LPS was acquired in the positive ion mode, a similar pattern of signals was detected (Figure 1b).

To further confirm the structure of the lipid A constituents, LID-MS/MS analysis of some ions were performed. Among them, LID-MS/MS spectrum of *m/z* 2225.10 (Figure 2a) showed ions at *m/z* 2165.28 (calc. *m/z* 2165.4139; $C_{110}H_{210}N_4Na_3O_{26}P_3^{+\cdot}$), *m/z* 2123.03 (calc. *m/z* 2123.5106; $C_{112}H_{216}N_5Na_2O_{24}P_2^{+}$), and *m/z* 2057.77 (calc. *m/z* 2058.4786; $C_{110}H_{211}N_4NaO_{24}P_2^{+\cdot}$) that correspond to the loss of an ethanolamine group, a sodium phosphate group, and a sodium phosphorylethanolamine group, respectively. Accordingly, fragment ions ascribed to tetra-, tri-, and di-acylated species substituted with one P and one PPEA group were detected (*Escherichia coli* 1). In the low mass range, diagnostic ions generated after laser-induced cleavage of the glycosidic linkage between the two GlcN3N units within the lipid backbone [28–30] confirmed the structure. Thus, the oxonium ion at *m/z* 827.99 (calc. *m/z* 827.5521; $C_{42}H_{81}N_2NaO_{10}P^{+}$) is compatible with the GlcN3N II unit acylated with C16:0 (3-OH) and C20:0 (3-OH) fatty acids carrying one sodium phosphoryl group. The complement fragment ion at *m/z* 940.05 (calc. *m/z* 940.5599; $C_{42}H_{85}N_3NaO_{14}P_2^{+}$) indicates the presence of a PPEA group substituting the GlcN3N I unit, acylated with C16:0 (3-OH) and C18:0 (3-OH) fatty acids.

The LID-MS/MS spectrum of the parent ion *m/z* 2037.12 (Figure 2b, Table 2) showed a signal at *m/z* 1978.39 in agreement with the loss of an ethanolamine group. The signal at *m/z* 1918.63 matches the loss of a sodium PPEA group, and the ion at *m/z* 1494.67 corresponds to the loss of a PEA group concomitant with a C14:0 (3-OC16:0) as ketene. Similarly, the ion at *m/z* 1240.35 agrees with the loss of a sodium PEA group, a C16:0 (3-OC12:0) and a C16:0, both of them as ketenes.

Further on, the MALDI-TOF mass spectrum acquired in the negative ion mode of *B. suis* lipid A using gentisic acid as matrix was performed (Figure 3a, Table 3). The spectrum showed in the high mass region, the ion at *m/z* 2223.32 analogous to the signal at *m/z* 2225.10 obtained in the positive ion mode. In addition, the loss of a sodium phosphate group gave rise to the ion at *m/z* 2121.65. Also, a main cluster of ions ranging from *m/z* 1950 to 2040 indicates the presence of hexa-acylated species containing the diGlcN3N backbone attached to a phosphate group with Δ 14 Da, attributable to differences in the acyl groups. Thus, among them, the most intense peak at *m/z* 1994.54 (calc. *m/z* 1994.5908; $C_{114}H_{218}N_4O_{20}P^{-}$) bears three C16:0 (3-OH), one C18:0 (3-OH), one C20:0 (3-OH), and one C16:0 fatty acids. Accordingly, a penta-acylated species at *m/z* 1756.03 (calc. *m/z* 1756.3611; $C_{98}H_{188}N_4O_{19}P^{-}$) was detected. In the low mass range, the ion at *m/z* 1394.46 (calc. *m/z* 1394.8242; $C_{64}H_{127}N_5O_{21}P_3^{-}$) is consistent with the tri-acylated diGlcN3N backbone carrying one P group and one PPEA group.

In order to assure the new feature, MALDI-LID-MS/MS analysis in the negative ion mode of the parent ion *m/z* 2223.32

Table 2. Proposed structures for the ion *m/z* 2037 and fragment ions obtained from *Brucella suis* Lipid A after MALDI- LID-MS/MS analysis in the positive ion mode. Sugar backbone: [GlcN3N-GlcN3N]

$Mass_{calc.}$[a] $[M+Na]^+$	$Mass_{meas}$[b] $[M+Na]^+$		Proposed structures	P	EtN
2037.3799	2037.12	$C_{104}H_{202}N_5NaO_{25}P_3^{+}$	C16:0(3-OC16:0) C14:0(3-OC16:0) C16:0(3-OC12:0)	3	1
1977.3345	1978.39	$C_{102}H_{196}N_4NaO_{24}P_3^{+}$	C16:0(3-OC16:0) C14:0(3-OC16:0) C16:0(3-OC12:0)	3	-
1919.3501	1918.63	$C_{102}H_{194}N_4Na_2O_{21}P_2^{+\cdot}$	C16:0(3-OC16:0) C14:0(3-OC16:0) C16:0(3-OC12:0)	2	-
1493.9118	1494.67	$C_{72}H_{138}N_4Na_3O_{19}P_2^{+}$	C16:0(3-OC16:0) C16:0(3-OC12:0)	2	-
1239.7496	1240.35	$C_{58}H_{114}N_4NaO_{18}P_2^{+}$	C16:0(3-OC16:0) C14:0	2	-

[a]calc: calculated monoisotopic masses.
[b]meas: measured.
GlcN3N: 2,3-diamino-2,3-dideoxyglucose; P: phosphate; EtN: ethanolamine

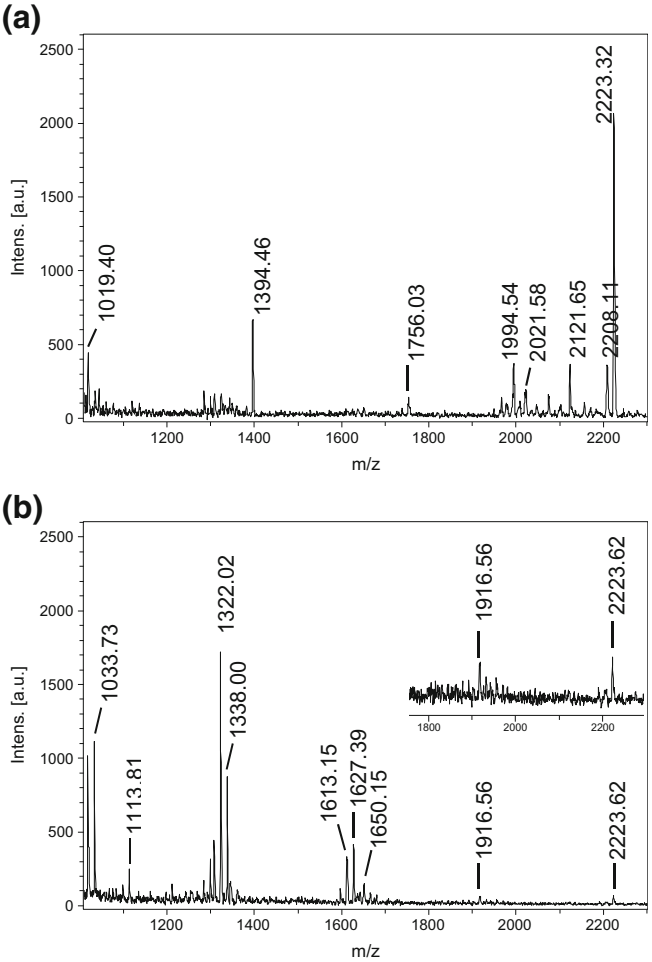

Figure 3. MALDI-TOF mass spectra acquired in the negative ion mode using gentisic acid as matrix. **(a)** Mass spectrum of *B. suis* lipid A. **(b)** Mass spectrum of *B. abortus* lipid A. Inset: magnification of region *m/z* 1700–2300

(Figure 4a, Table 3) was performed. Thus, the fragment ions at *m/z* 2157.52, *m/z* 2120.58, and *m/z* 2056.01 correspond to the loss of $NH_2CH_2CH_2^{\cdot}$, of a NaP, and a sodium PEA, respectively, from the parent ion. Also, losses of acyl groups were detected. Thus, *m/z* 1473.02 was ascribed to the loss of C18:0 (3-OH) as ketene, a C12:0 fatty acid, a PEA, and one P from *m/z* 2223.32. In accordance, the loss of C16:0 (3-OC16OH) and sodium PEA group from *m/z* 2223.32 yielded *m/z* 1429.08. On the other hand, the ion at *m/z* 1392.11 shows the loss of a P from ion *m/z* 1473.02. Ions at *m/z* 1147.80 and *m/z* 1129.64 (ΔH_2O) correspond to the loss of a C16:0 (3-OH) as ketene/acid, concomitant with the loss of a C16:0 (3-OC12OH) and a C18:0 (3-OH) as ketenes and a NaP from the parent ion.

In addition, the fragment ions at *m/z* 727.33 (calc. *m/z* 727.4264; $C_{32}H_{64}N_4O_{12}P^-$) and *m/z* 647.21 (calc. *m/z* 647.4595; $C_{32}H_{63}N_4O_9^-$) (Δ 80 Da) consist of the diGlcN3N backbone carrying one C20:0 (3-OH) and a phosphate group; and *m/z* 682.34 (calc. *m/z* 682.3685; $C_{30}H_{57}N_3O_{12}P^-$) consists of the diGlcN3N backbone after the loss of ammonia carrying C18:0 (3-OH) and a phosphate group. These last ions indicate the presence of C20:0 (3-OH) and C18:0 (3-OH), both linked to the diGlcN3N backbone. In the low mass range, diagnostic ions at *m/z* 78.65 and 96.65 account for the presence of phosphate groups and ions at *m/z* 282.37 and 327.44 confirm the presence of 3-hydroxyoctadecanoic acid and 3-hydroxyeicosanoic acid, respectively.

As expected, MALDI-LID-MS/MS spectrum of the precursor ion *m/z* 2120.58 (Figure 4b, Table 4) showed below *m/z* 1500 a similar fragmentation profile as *m/z* 2223.32. In accordance, the fragment ions at *m/z* 2061.52 and *m/z* 1953.62 correspond to the loss of ethanolamine and PEA, respectively, from the parent ion. In addition, the fragment ion *m/z* 1568.94 attributed to the loss of C16:0 (3-OC16OH) as ketene also from the parent ion. Further loss of C16:0 (3-OC12) as ketene from the latter gave rise to the fragment ion *m/z* 1177.48. Moreover, the ion at *m/z* 622.28 (calc. *m/z* 621.2562; $C_{24}H_{46}N_3NaO_{10}P_2^{-\cdot}$) corresponds to a GlcN3N residue carrying a PPEA group and anhydroC16:0 (3-OH). In addition, diagnostic fragment ions corresponding to phosphate (80 Da; 96 Da) and a pyrophosphate group ($H_3O_6P_2^-$; 160 Da) were detected [31].

It has been reported that *B. abortus* lipid A presents mono- and diphosphorylated acylated diGlcN3N structures [22, 23]. However, when the mass spectrum of *B. abortus* lipid A acquired in the negative ion mode was analyzed, the ion at *m/z* 2223.62 (calc. *m/z* 2223.4438, $C_{112}H_{214}N_5Na_3O_{27}P_3^-$)

Table 3. Proposed structures for the ion *m/z* 2223.32 and fragment ions obtained from *Brucella suis* lipid A after MALDI- LID-MS/MS analysis in the negative ion mode. Sugar backbone: [GlcN3N-GlcN3N]

$Mass_{calc.}$[a] $[M–H]^-$	$Mass_{meas}$[b] $[M–H]^-$		Proposed structures	P	EtN
2223.4438	2223.32	$C_{112}H_{214}N_5Na_3O_{27}P_3^-$	C16:0(3-OC16:0 3-OH); C20:0(3-OH); C16:0(3-OC12:0); C18:0(3-OH)	3	1
2158.4196	2157.52	$C_{110}H_{210}N_4Na_2O_{27}P_3^-$	C16:0(3-OC16:0 3-OH); C20:0(3-OH); C16:0(3-OC12:0); C18:0(3-OH)	3	-
2121.4955	2120.58	$C_{112}H_{214}N_5Na_2O_{24}P_2^-$	C16:0(3-OC16:0 3-OH); C20:0(3-OH); C16:0(3-OC12:0); C18:0(3-OH)	2	1
2056.4713	2056.01	$C_{110}H_{210}N_4NaO_{24}P_2^-$	C16:0(3-OC16:0 3-OH); C20:0(3-OH); C16:0(3-OC12:0); C18:0(3-OH)	2	-
1472.0896	1473.02	$C_{80}H_{152}N_4O_{17}P^-$	C16:0(3-OC16:0 3-OH); C20:0(3-OH); C16:0*	1	-
1429.0712	1429.08	$C_{78}H_{149}N_4O_{16}P^{\cdot-}$	C20:0(3-OH); C16:0(3-OC12:0); C18:0(3-OH)	1	-
1392.1232	1392.11	$C_{80}H_{151}N_4O_{14}P^-$	C16:0(3-OC16:0 3-OH); C20:0(3-OH); C16:0*	-	-
1148.6234	1147.80	$C_{50}H_{98}N_5Na_2O_{17}P_2^-$	C16:0(3-OH); C20:0(3-OH)	2	1
1130.6128	1129.64	$C_{50}H_{96}N_5Na_2O_{16}P_2^-$	C16:0*; C20:0(3-OH)	2	1

[a]calc: calculated monoisotopic masses.
[b]meas: measured. GlcN3N: 2,3-diamino-2,3-dideoxyglucose.
P: phosphate; EtN: ethanolamine; C16:0*: Δ^3-hexadecenoyl residue.

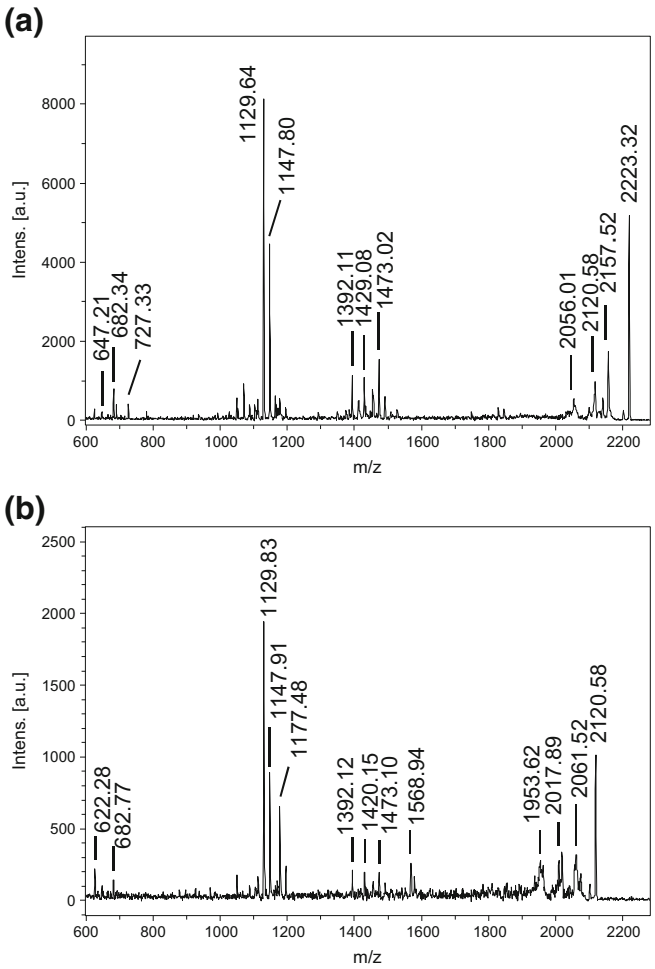

Figure 4. **(a)** MALDI-LID-MS/MS spectrum of parent ion *m/z* 2223.32 from Figure 3. **(b)** MALDI-LID-MS/MS spectrum of parent ion *m/z* 2120.58 from Figure 3

although in low intensity, was also detected (Figure 3b). As described above, this ion confirms the presence of one P group and one PPEA group in the structure. In accordance, the ion at *m/z* 1916.56 (1917.3465; $C_{100}H_{193}N_5NaO_{23}P_2^-$) corresponds to a penta-acylated diGlcN3N backbone also carrying a PPEA group. In addition, a cluster of ions ranging from *m/z* 1680 to 1595 with main ion at *m/z* 1627.39 (1628.2410, $C_{90}H_{172}N_4O_{18}P^-$) corresponds to penta-acylated species carrying one phosphate group. Another cluster of ions in the range *m/z* 1350–1280 with main ion at *m/z* 1322.02 (1321.8289; $C_{64}H_{124}N_4NaO_{18}P_2^-$) was ascribed to the tri-acylated diGlcN3N backbone substituted with one pyrophosphate group or two phosphate groups. Di-acylated species with hexadecanoyl 3-hydroxy and octadecanoyl 3-hydroxy fatty acids carrying one phosphate and one pyrophosphate group at *m/z* 1113.81 (calc. *m/z* 1113.5523; $C_{46}H_{92}N_4O_{20}P_3^-$), and two phosphate groups at *m/z* 1033.73 (*m/z* 1033.5860; $C_{46}H_{91}N_4O_{17}P_2^-$), were also detected.

Conclusions

Brucella harbors a peculiar nonclassic LPS in comparison to classic LPS from enterobacteria such as *E. coli* [4], and it has been described that the lipid A, linked to the core oligosaccharide, contains 2,3 diamino-2,3,-dideoxy-D-glucose (diaminoglucose) as backbone substituted with amide and ester linked long chain saturated and hydroxylated fatty acids [21]. The hydrophobic lipid A region constitutes mostly the outer coating of the outer membrane and is responsible for many of the endotoxic properties attributed to LPS [18]. Dramatic differences on the lipid A profiles of R and S *Brucella abortus* strains compared with *E. coli* have already been reported [23]. MALDI-TOF mass spectra of *B. abortus* lipid A showed a cluster of ions at high mass range that was ascribed to hepta-acylated species not detected before. However, under the light of our results obtained by MALDI-TOF MS and confirmed by MALDI-LID-MS/MS analysis, these signals correspond to hexa-acylated species substituted with one P and one PPEA group.

It is known that one mechanism of antimicrobial peptide resistance is to modify the cell surface with positively charged moieties, which results in electrostatic repulsion of the positively charged antimicrobial peptides [32]. Frequently, gram-negative bacteria modify their lipopolysaccharide with positively charged aminoarabinose or PEA and these modifications affect virulence [33, 34]. For example, it has been reported that the modification of lipid A with PEA increases resistance of *N. gonorrhoeae* to complement killing and survival of both gonococci and meningococci in vivo [35]. PEA modification of Lipid A in *Salmonella enterica* serovar *Typhimurium* and *E. coli* strains has also been well documented [36].

Table 4. Proposed structures for the ion *m/z* 2121.65 and fragment ions obtained from *Brucella suis* Lipid A after MALDI- LID-MS/MS analysis in the negative ion mode. Sugar backbone: [GlcN3N-GlcN3N]

$Mass_{calc.}$[a] $[M-H]^-$	$Mass_{meas}$[b] $[M-H]^-$		Proposed structures	P	EtN
2121.4955	2121.65	$C_{112}H_{214}N_5Na_2O_{24}P_2^-$	C16:0(3-OC16:0 3-OH); C20:0(3-OH); C16:0(3-OC12:0); C18:0(3-OH)	2	1
2061.4505	2061.52	$C_{110}H_{208}N_4Na_2O_{23}P_2^{-}$	C16:0(3-OC16:0 3-OH); C20:0(3-OH); C16:0(3-OC12:0); C18:0(3-OH)	2	-
1954.5231	1953.62	$C_{110}H_{210}N_4O_{21}P^-$	C16:0(3-OC16:0 3-OH); C20:0(3-OH); C16:0(3-OC12:0); C18:0(3-OH)	1	-
1569.0824	1568.94	$C_{80}H_{156}N_5O_{20}P_2^-$	C20:0(3-OH); C16:0(3-OC12:0); C18:0(3-OH)	2	1
1176.6547	1177.48	$C_{52}H_{102}N_5Na_2O_{17}P_2^-$	C20:0(3-OH); C18:0(3-OH)	2	1

P: phosphate; EtN: ethanolamine.

The canine pathogen *Capnocytophaga canimorsus* and plant pathogens *Xanthomonas campestris* and *X. axonopodis* also modify their lipid A with PEA [37–39], which alters the innate immune responses they trigger, altering the disease manifestations. Thus, modification of lipid A by PEA as a means to evade the effects of antimicrobial agents by altering the electrostatic charge on the bacterial membrane is prevalent.

Furthermore, it has been reported that modifications of the lipid A can drastically alter its immunostimulatory ability as well as resistance to antibiotics. For example, the addition of positively charged residues, including ethanolamine, aminoarabinose, or glucosamine to lipid A, modulates CAMP resistance [40–42]. Colistin resistance has been linked to modifications of the lipid A of the LPS moiety from many bacterial species, including *A. Baumanii s*trains [43, 44]. In *Helicobacter pylori* modification of the lipid A is performed by a two-step process, removal of the 1-phosphate group by a phosphatase followed by the addition of a PEA residue, resulting in increased resistance to polymyxin [45].

Regarding pyrophosphorylethanolamine substitutions, the lipid A of *Campylobacter jejuni* is characterized by the presence of PEA linked to the phosphate group attached to the 1 and 4′ positions of the disaccharide backbone [46]. Conversely, the lipid A from *A. baumanniss* is both bisphosphorylated and pyrophosphorylated and substituted with a GalN unit at the 1-phosphate position and a PEA at the 4′phosphate position. Also, the PEA group was found to be attached to the lipid A backbone via a phosphodiester bond at either the C-4′ monophosphate or the C-1 monophosphate position [47].

The finding that *B. abortus* and *B. suis* contain one PPEA on their Lipid A moieties may open new possibilities of exploring the poorly elucidated set of mechanisms involved in *Brucellae* virulence that include the ability to escape prompt detection by innate immunity during the initial stages of the infectious process.

Acknowledgements

This work was supported by the Consejo Nacional de Investigaciones Científicas y Técnicas Grant PIP-11220110100660, Agencia Nacional de Promoción Científica y Tecnológica (ANPCyT) grant PICT-2013-0736 and PICT-2014-1028 and Universidad de Buenos Aires grant 20020130100476BA. The Ultraflex II (Bruker) TOF/TOF mass spectrometer was supported by ANPCyT grant PME 125 (CEQUIBIEM). A.S.C., J.E.U., and C.C. are members of Carrera de Investigador Científico y Tecnológico of CONICET.

References

1. Franco, M.P., Mulder, M., Smits, H.L.: Human brucellosis. Lancet Infect. Dis. **7**, 775–786 (2007)
2. Díaz-Aparicio, E., Aragón, V., Marín, C., Alonso, B., Font, M., Moreno, E., Pérez-Ortiz, S., Blasco, J.M., Díaz, R., Moriyón, I.: Comparative analysis of *Brucella* serotype A and M and *Yersinia enterocolitica* O:9 polysaccharides for serological diagnosis of brucellosis in cattle, sheep, and goats. J. Clin. Microbiol. **31**, 3136–3141 (1993)
3. Cloeckaert, A., Weynants, V., Godfroid, J., Verger, J.M., Grayon, M., Zygmunt, M.S.: O-polysaccharide epitopic heterogeneity at the surface of *Brucella* spp. studied by enzyme-linked immunosorbent assay and flow cytometry. Clin. Diagn. Lab. Immunol. **5**, 862–870 (1998)
4. Lapaque, N., Moriyon, I., Moreno, E., Gorvel, J.P.: Brucella lipopolysaccharide acts as a virulence factor. Curr. Opin. Microbiol. **8**, 60–66 (2005)
5. Conde-Alvarez, R., Arce-Gorvel, V., Gil-Ramirez, Y., Iriarte, M., Grillo, M.J., Gorvel, J.P., Moriyon, I.: Lipopolysaccharide as a target for brucellosis vaccine design. Microb. Pathog. **58**, 29–34 (2013)
6. Raetz, C.R., Whitfield, C.: Lipopolysaccharide endotoxins. Annu. Rev. Biochem. **71**, 635–700 (2002)
7. Valvano, M.A., Furlong, S.E., Patel, K.B.: In: Knirel, Y.A., Valvano, M.A. (eds.) Bacterial lipopolysaccharides. Springer-Verlag, Wien (2011)
8. Barquero-Calvo, E., Chaves-Olarte, E., Weiss, D.S., Guzmán-Verri, C., Chacón-Díaz, C., Rucavado, A., Moriyón, I., Moreno, E.: *Brucella abortus* uses a stealthy strategy to avoid activation of the innate immune system during the onset of infection. PLoS ONE. **2**, e631 (2007)
9. Bundle, D.R., Cherwonogrodzky, J.W., Perry, M.B.: Structural elucidation of the *Brucella melitensis* M antigen by high-resolution NMR at 500 MHz. Biochemistry. **26**, 8717–8726 (1987)
10. Bundle, D.R., Cherwonogrodzky, J.W., Perry, M.B.: The structure of the lipopolysaccharide O-chain (M antigen) and polysaccharide B produced by *Brucella melitensis* 16M. FEBS Lett. **216**, 2611–2647 (1987)
11. Meikle, P.J., Perry, M.B., Cherwonogrodzky, J.W., Bundle, D.R.: Fine structure of A and M antigens from *Brucella* biovars. Infect. Immun. **57**, 2820–2828 (1989)
12. Cherwonogrodzky, J.W., Perry, M.B., Bundle, D.R.: Identification of the A and M antigens of *Brucella* as the O-polysaccharides of smooth lipopolysaccharides. Can. J. Microbiol. **33**, 979–981 (1987)
13. Kubler-Kielb, J., Vinogradov, E.: Reinvestigation of the structure of *Brucella* O-antigens. Carbohydr. Res. **378**, 144–147 (2013)
14. Conde-Alvarez, R., Arce-Gorvel, V., Iriarte, M., Mancek-Keber, M., Barquero-Calvo, E., Palacios-Chaves, L., Chacón-Díaz, C., Chaves-Olarte, E., Martirosyan, A., von Bargen, K., Grilló, M-J., Jerala, R., Brandenburg, K., Llobet, E., Bengoechea, J.A., Moreno, E., Moriyón, I., Gorvel, J.-P.: The lipopolysaccharide core of *Brucella abortus* acts as a shield against innate immunity recognition. PLoS Pathog **8**, e1002675 (2012).
15. Kubler-Kielb, J., Vinogradov, E.: The study of the core part and non-repeating elements of the O-antigen of *Brucella* lipopolysaccharide. Carbohydr. Res. **366**, 33–37 (2013)
16. Gil-Ramírez, Y., Conde-Álvarez, R., Palacios-Chaves, L., Zúñiga-Ripa, A., Grilló, M.J., Arce-Gorvel, V., Hanniffy, S., Moriyón, I., Iriarte, M.: The identification of wadB, a new glycosyltransferase gene, confirms the branched structure and the role in virulence of the lipopolysaccharide core of *Brucella abortus*. Microb. Pathog. **73**, 53–59 (2014)
17. Fontana, C., Conde-Álvarez, R., Ståhle, J., Holst, O., Iriarte, M., Zhao, Y., Arce-Gorvel, V., Hanniffy, S., Gorvel, J.P., Moriyón, I., Widmalm, G.: Structural studies of lipopolysaccharide-defective mutants from *Brucella melitensis*. Identify a core oligosaccharide critical in virulence. J. Biol. Chem. **291**, 7727–7741 (2016)
18. Raetz, C.R.H.: Bacterial lipopolysaccharides: a remarkable family of bioactive macroamphiphiles**.** In *Escherichia coli* and *Salmonella* Vol. 1. Neidhardt, F.C., Ed. Cell. Mol. Biol. 1035–1063 (1996)
19. Ramos-Sánchez, M.C., Orduña-Domingo, A., Rodríguez Tones, A., Martin-Gil, F.J., Martin-Gil, J.: Investigations on thermotropic phase behavior of lipids A from *Brucella* and other gram-negative bacteria. Thermochim. Acta. **144**, 299–305 (1992)
20. Rojas, N., Freer, E., Weintreub, A., Ramirez, M., Lind, S., Moreno, E.: Immunochemical identification of *Brucella abortus* lipopolysaccharide epitopes. Clin. Diagn. Lab. Immunol. **1**, 206–213 (1994)
21. Moreno, E., Stackebrandt, E., Dorsch, M., Wolters, J., Busch, M., Mayer, H.: *Brucella abortus* 16S rRNA and lipid A reveal phylogenetic relationship with members of the alpha-2 subdivision of the class proteobacteria. J. Bacteriol. **172**, 3569–3576 (1990)
22. Qureshi, N., Takayama, K., Seydel, U., Wang, R., Cotter, R.J., Agrawal, P.K., Bush, C.A., Kurtz, R., Berman, T.: Structural analysis of the Lipid A derived from the polysaccharide of *Brucella abortus*. J. Endotoxin Res. **1**, 137–148 (1994)
23. Cardoso, P.G., Macedo, G.C., Azevedo, V., Oliveira, S.C.: *Brucella* spp noncanonical LPS: structure, biosynthesis, and interaction with host immune system. Microbial Cell Factories. **5**, 13–43 (2006)

24. Chain, P.S., Comerci, D.J., Tolmasky, M.E., Larimer, F.W., Malfatti, S.A., Vergez, L.M., Aguero, F., Land, M.L., Ugalde, R.A., Garcia, E.: Whole-genome analyses of speciation events in pathogenic brucellae. Infect. Immun. **73**, 8353–8361 (2005)
25. Paulsen, I.T., Seshadri, R., Nelson, K.E., Eisen, J.A., Heidelberg, J.F., Read, T.D., Dodson, R.J., Umayam, L., Brinkac, L.M., Beanan, M.J., Daugherty, S.C., Deboy, R.T., Durkin, A.S., Kolonay, J.F., Madupu, R., Nelson, W.C., Ayodeji, B., Kraul, M., Shetty, J., Malek, J., Van Aken, S.E., Riedmuller, S., Tettelin, H., Gill, S.R., White, O., Salzberg, S.L., Hoover, D.L., Lindler, L.E., Halling, S.M., Boyle, S.M., Fraser, C.M.: The *Brucella suis* genome reveals fundamental similarities between animal and plant pathogens and symbionts. Proc. Natl. Acad. Sci. USA. **99**, 13148–13153 (2002)
26. Luederitz, O., Risse, H.J., Schulte-Holthausen, H., Strominger, J.L., Sutherland, I.W., Westphal, O.: Biochemical studies of the smooth-rough mutation in *Salmonella minnesota*. J. Bacteriol. **89**, 343–354 (1965)
27. Osborn, M.J.: Studies on the gram-negative cell wall. Evidence for the role of 2-keto-3-deoxyoctonate in the lipopolysaccharide of *Salmonella typhimurium*. Proc. Natl. Acad. Sci. USA. **50**, 499–506 (1963)
28. Choma, A., Sowinski, P.: Characterization of *Mesorhizobium huakuii* lipid A containing both D-galacturonic acid and phosphate residues. Eur. J. Biochem. **271**, 1310–1322 (2004)
29. Rund, S., Lindner, B., Brade, H., Holst, O.: Structural analysis of the lipopolysaccharide from *Chlamydophila psittaci* strain 6BC. Eur. J. Biochem. **267**, 5717 (2000)
30. Gudlavalleti, S.K., Forsberg, L.S.: Structural characterization of the lipid A component of *Sinorhizobium* sp. NGR234 rough and smooth form lipopolysaccharide. Demonstration that the distal amide-linked acyloxyacyl residue containing the long chain fatty acid is conserved in *Rhizobium* and *Sinorhizobium* sp. J. Biol. Chem. **278**, 3957–3968 (2003)
31. Jones, J.W., Shaffer, S.A., Ernst, R.K., Goodlett, D.R., Turecek, F.: Determination of pyro-phosphorylated forms of lipid A in gram-negative bacteria using a multivaried mass spectrometric approach. PNAS. **105**(**35**), 12742–12747 (2008)
32. Gunn, J.S.: Bacterial modification of LPS and resistance to antimicrobial peptides. J. Endotoxin Res. **7**, 57–62 (2001)
33. Tamayo, R., Choudhury, B., Septer, A., Merighi, M., Carlson, R., Gunn, J.S.: Identification of *cpt A*, a PmrA-regulated locus required for phosphoethanolamine modification of the *Salmonella enterica* serovar Typhimurium lipopolysaccharide core. J. Bacteriol. **187**, 3391–3399 (2005)
34. Cox, A.D., Wright, J.C., Li, J., Hood, D.W., Moxon, E.R., Richards, J.C.: Phosphorylation of the lipid A region of meningococcal lipopolysaccharide: identification of a family of transferases that add phosphoethanolamine to lipopolysaccharide. J. Bacteriol. **185**, 3270–3277 (2003)
35. Shafer, W.M., Dutta Ray, T., Ram, S.: Phosphoethanolamine residues on the lipid A moiety of *Neisseria gonorrhoeae* lipooligosaccharide modulate binding of complement inhibitors and resistance to complement killing. Infect Immun. **81**, 33–42 (2013)
36. Falagas, M.E., Rafailidis, P.I., Matthaiou, D.K.: Resistance to polymyxins: mechanisms, frequency and treatment options. Drug Resist. Update. **13**, 132–138 (2010)
37. Ittig, S., Lindner, B., Stenta, M., Manfredi, P., Zdorovenko, E., Knirel, Y.A., dal Peraro, M., Cornelis, G.R., Zahringer, U.: The lipopolysaccharide from *Capnocytophaga canimorsus* reveals an unexpected role of the core oligosaccharide in MD-2 binding. PLoS Pathog. **8**, e1002667 (2012)
38. Silipo, A., Sturiale, L., Garozzo, D., Erbs, G., Jensen, T.T., Lanzetta, R., Dow, J.M., Parrilli, M., Newman, M.A., Molinaro, A.: The acylation and phosphorylation pattern of lipid A from *Xanthomonas campestris* strongly influence its ability to trigger the innate immune response in Arabidopsis. Chembiochem. **9**, 896–904 (2008)
39. Casabuono, A.C., Petrocelli, S., Ottado, J., Orellano, E.G., Couto, A.S.: Structural analysis and involvement in plant innate immunity of *Xanthomona axonopodis* citri lipopolysaccharide. J. Biol. Chem. **286**(29), 25628–25643 (2011)
40. Basheer, S.M., Guiso, N., Tirsoaga, A., Caroff, M., Novikov, A.: Structural modifications occurring in lipid A of *Bordetella bronchiseptica* clinical isolates as demonstrated by matrix-assisted laser desorption/ionization time-of-flight mass spectrometry. Rapid Commun. Mass Spectrom. **25**, 1075–1081 (2011)
41. Llobet, E., Campos, M.A., Gimenez, P., Moranta, D., Bengoechea, J.A.: Analysis of the networks controlling the antimicrobial-peptide-dependent induction of *Klebsie lla pneumoniae* virulence factors. Infect. Immun. **79**, 3718–3732 (2011)
42. Moskowitz, S.M., Ernst, R.K., Miller, S.I.: PmrAB, a two-component regulatory system of *Pseudomonas aeruginosa* that modulates resistance to cationic antimicrobial peptides and addition of amino-arabinose to lipid A. J. Bacteriol. **186**, 575–579 (2004)
43. Beceiro, A., Llobet, E., Aranda, J., Bengoechea, J.A., Doumith, M., Hornsey, M., Dhanji, H., Chart, H., Bou, G., Livermore, D.M., Woodford, N.: Phosphoethanolamine modification of lipid A in colistin-resistant variants of *Acinetobacter baumannii* mediated by the -*pmr*AB two-component regulatory system. Antimicrob. Agents Chemother. **55**, 3370–3379 (2011)
44. Arroyo, L.A., Herrera, C.M., Fernandez, L., Hankins, J.V., Trent, M.S., Hancock, R.E.: The *pmr*CAB operon mediates polymyxin resistance in *Acinetobacter baumannii* ATCC 17978 and clinical isolates through phosphoethanolamine modification of lipid A. Antimicrob. Agents Chemother. **55**, 3743–3751 (2011)
45. Herrera, C.M., Hankins, J.V., Trent, M.S.: Activation of PmrA inhibits LpxT-dependent phosphorylation of lipid A promoting resistance to antimicrobial peptides. Mol. Microbiol. **76**, 1444–1460 (2010)
46. Cullen, T.W., Trent, M.S.: A link between the assembly of flagella and lipooligosaccharide of the gram-negative bacterium *Campylobacter jejuni*. Proc. Natl. Acad. Sci. USA. **107**(11), 5160–5165 (2010)
47. Pelletier, M.R., Casella, L.G., Jones, J.W., Adams, M.D., Zurawski, D.V., Hazlett, K.R., Doi, Y., Ernst, R.K.: Unique structural modifications are present in the lipopolysaccharide from colistin-resistant strains of *Acinetobacter baumannii*. Antimicrob. Agents Chemother. **57**(10), 4831–4840 (2013)